

1  **$\beta$ -catenin has both conserved and novel functions in the sponge *Ephydatia muelleri***

2

3 Authors:

4 Klaske J. Schippers<sup>1,2</sup> and Scott A. Nichols<sup>1</sup>

5

6 Affiliations:

7 1. Biological Sciences, University of Denver, 2101 E. Wesley Ave, Denver, CO 80208, USA

8 2. Current address: EMBL, Meyerhofstrasse 1, 67117, Heidelberg, Germany

9

10 Corresponding author:

11 Scott. A. Nichols (scott.nichols@du.edu)

12

## 1 **ABSTRACT**

2  $\beta$ -catenin acts as a transcriptional co-activator in the Wnt/ $\beta$ -catenin signaling pathway and a  
3 cytoplasmic effector in cadherin-based cell adhesion. These functions are ancient within  
4 animals, but the earliest steps in  $\beta$ -catenin evolution remain unresolved due to limited data from  
5 key lineages -- sponges, ctenophores and placozoans. Previous studies in sponges have  
6 characterized  $\beta$ -catenin expression dynamics and have ectopically activated the Wnt pathway  
7 through pharmacological inhibition of GSK3 $\beta$ , a negative regulator of  $\beta$ -catenin. However, both  
8 approaches rely upon untested assumptions about the conservation of  $\beta$ -catenin function and  
9 regulation in sponges. Here, we test these assumptions using a custom antibody raised against  
10  $\beta$ -catenin from the sponge *Ephydatia muelleri*. We find that cadherin-complex genes co-  
11 precipitate with Em $\beta$ catenin from endogenous cell lysates, but that Wnt pathway components do  
12 not. However, through immunostaining we detect both cell boundary and nuclear populations,  
13 and we find evidence that Em $\beta$ catenin is a conserved substrate of GSK3 $\beta$ . Collectively, these  
14 data support the conservation of Em $\beta$ catenin in adhesion and signaling. In addition to its  
15 conserved functions shared with bilaterians, we also find evidence for an entirely novel  
16 Em $\beta$ catenin function. Em $\beta$ catenin localizes to the distal ends of F-actin stress fibers in focal  
17 adhesion-like structures (typically integrin-based adhesions) in the substrate-attachment  
18 epithelium. This finding suggests a fundamental difference in  $\beta$ -catenin function and in the cell  
19 adhesion mechanisms operating in sponge versus bilaterian tissues.

20

## 21 **INTRODUCTION**

22 A well-known pattern in the fossil record is the appearance of most animal lineages over a  
23 relatively short time interval (between 541-485 Mya) during the Cambrian. Many of the  
24 characteristics that define and distinguish modern animals from each other had already evolved  
25 by the time that these first body fossils appear, leaving few clues about either the process or  
26 sequence of animal body plan diversification. As a result, our understanding of the earliest  
27 events in animal evolution rests largely upon the comparative study of extant organisms. The  
28 rationale for this approach is that body plan differences between living organisms reflect  
29 accumulated evolutionary changes to their underlying cell and developmental biology.

30

31 For practical reasons, large research communities have established around a handful of  
32 biomedical research models such as mouse, fruit fly, roundworm and zebrafish. Data from these  
33 few organisms largely form the basis for textbook generalizations about animal biology, and  
34 ultimately have contributed to a bilaterian-biased perspective on animal evolution. However, to

1 study the deepest periods of animal ancestry, it will be critical to incorporate data from non-  
2 bilaterian animals such as sponges and ctenophores (Dunn, et al. 2015). Non-bilaterians are  
3 more phylogenetically divergent from each other, and from other animals, than are any of the  
4 biomedical research models listed above (Dohrmann and Wörheide 2017; Schuster, et al.  
5 unpublished data) but a lack of detailed mechanistic knowledge about their cell and  
6 developmental biology is currently limiting. However, progress in this area has accelerated due  
7 to advances in comparative genomics, with the initially surprising result that starkly different  
8 organisms share highly conserved developmental regulatory genes (McGinnis, et al. 1984;  
9 Kusserow, et al. 2005; Technau, et al. 2005; Nichols, et al. 2006). An important part of  
10 understanding animal body plan evolution will be to explain how conserved bilaterian regulatory  
11 genes/pathways function in non-bilaterian animals, how they may have functioned ancestrally,  
12 and how changes to their functions may have contributed to morphological evolution.

13

14 To begin to address these questions, the pleiotropic gene  $\beta$ -catenin is of considerable interest  
15 because it has pivotal roles in developmentally important processes ranging from cell adhesion  
16 to transcriptional regulation in the Wnt/ $\beta$ -catenin signaling pathway. In cell adhesion,  $\beta$ -catenin  
17 interacts with the cytoplasmic tail of cadherin receptors and with  $\alpha$ -catenin, an unrelated protein  
18 that links the adhesion complex to the actin cytoskeleton (Huber and Weis 2001; Shapiro 2009).  
19 This molecular complex forms the foundation of adherens junctions (AJs), and functions as the  
20 primary cell-cell adhesion mechanism in all studied bilaterian tissues, including epithelial tissues  
21 where AJs also serve as a spatial cue for the establishment of tissue polarity (Capaldo and  
22 Macara 2007). In Wnt/ $\beta$ -catenin signaling,  $\beta$ -catenin is a downstream effector that translocates  
23 to the nucleus in response to Wnt signals, where it forms a complex with the transcription factor  
24 TCF/Lef. Wnt/ $\beta$ -catenin signaling regulates hundreds of downstream target genes and is  
25 involved in developmental processes ranging from stem cell maintenance and renewal to axial  
26 patterning and gastrulation (Clevers and Nusse 2012).

27

28 An early study of  $\beta$ -catenin evolution in the sea anemone *Nematostella vectensis* predicted that  
29 the dual signaling and adhesion functions of  $\beta$ -catenin were ancient, and already established in  
30 early animal ancestors (Schneider, et al. 2003). Consistent with this view, it has since been  
31 established that not only  $\beta$ -catenin, but most components of the cadherin/catenin adhesion  
32 complex and the Wnt/ $\beta$ -catenin pathway are conserved in other non-bilaterian lineages as well.  
33 Moreover, expression studies suggest roles for Wnt/ $\beta$ -catenin in developmental patterning  
34 [reviewed in (Holstein 2012)] in cnidarians (Hobmayer, et al. 2000; Wikramanayake, et al. 2003;

1 Lee, et al. 2006; Momose, et al. 2008), ctenophores (Pang, et al. 2010; Jager, et al. 2013) and  
2 sponges (Adamska, et al. 2010; Leininger, et al. 2014), and based upon immunological and  
3 biochemical data, the cadherin/catenin adhesion complex appears to have conserved roles in  
4 epithelial cell adhesion in *N. vectensis* (Clarke, et al. 2016).

5  
6 Among non-bilaterian animals, studies of  $\beta$ -catenin in sponges are particularly of interest  
7 because their body plan differs significantly from other animals. With respect to the possibility of  
8 a conserved Wnt/ $\beta$ -catenin signaling pathway and how it might function in development, the  
9 adult sponge body plan lacks any clear axial polarity and it is contentious as to whether they  
10 undergo any developmental process with homology to gastrulation during embryogenesis  
11 (Nakanishi, et al. 2014); both axial patterning and gastrulation are hypothesized to be ancestral  
12 roles of Wnt/ $\beta$ -catenin signaling. With respect to a possible role for  $\beta$ -catenin in cadherin-based  
13 adhesion in sponges, ultrastructural studies suggest their tissues generally lack prominent and  
14 widespread AJs (Leys, et al. 2009). Instead, sponge cell adhesion (at least in demosponges)  
15 has long been attributed to a secreted glycoprotein complex called the Aggregation Factor  
16 (Henkart, et al. 1973; Müller and Zahn 1973; Fernández-Busquets and Burger 1997; Grice, et  
17 al. 2017), contributing to the view that sponge tissues are fundamentally different from other  
18 animal epithelia.

19  
20 Several studies have begun to address the function of  $\beta$ -catenin in sponges. In both the  
21 demosponge *Amphimedon queenslandica* and in the calcareous sponge *Sycon ciliatum*,  $\beta$ -  
22 catenin and other Wnt pathway components are dynamically expressed during embryonic  
23 development, suggesting a conserved role in developmental patterning (Adamska, et al. 2010;  
24 Leininger, et al. 2014). In adult tissues of *S. ciliatum*,  $\beta$ -catenin is also expressed in the  
25 choanoderm (feeding epithelium) and in a ring of migratory cells around the osculum (exhalant  
26 canal).

27  
28 Other studies have taken a pharmacological approach to study the function of Wnt/ $\beta$ -catenin  
29 signaling by treating the sponges with Glycogen Synthase Kinase 3 Beta (GSK3 $\beta$ ) inhibitors.  
30 GSK3 $\beta$  is a negative regulator of Wnt signaling that functions by phosphorylating free cytosolic  
31  $\beta$ -catenin, causing its ubiquitination and degradation by the proteasome. When GSK3 $\beta$  is  
32 inhibited (i.e., in the presence of Wnt ligands), cytosolic  $\beta$ -catenin accumulates, translocates to  
33 the nucleus and activates TCF/Lef and the transcription of Wnt target genes. A study by  
34 Lapébie and colleagues (2009) reported that GSK3 $\beta$  inhibitors caused the homoscleromorph

1 sponge *Oscarella lobularis* to develop ectopic ostia (incurrent water pores) and caused  
2 morphological changes to the exopinacoderm (outer epithelium), suggesting a role for Wnt/ $\beta$ -  
3 catenin signaling in sponge epithelial morphogenesis. Another study by Windsor and Leys  
4 (2010) reported that treating the freshwater demosponge *Ephydatia muelleri* with GSK3 $\beta$   
5 inhibitors resulted in the formation of ectopic oscula (exhalant water canals) and malformed  
6 choanocyte chambers (filter feeding epithelia), suggesting that the Wnt/ $\beta$ -catenin pathway plays  
7 a role in establishing the aquiferous system in sponges.

8  
9 With respect to the possible role of  $\beta$ -catenin in cadherin-based adhesion in sponges, all AJ  
10 components have been identified (Srivastava, et al. 2010; Nichols, et al. 2012; Riesgo, et al.  
11 2014), but experimental evidence for their function is limited. Sequence analyses and structural  
12 predictions indicate that sponge homologs of  $\beta$ -catenin and classical cadherins are sufficiently  
13 similar to their bilaterian counterparts to suggest conserved protein interactions. From an  
14 experimental perspective, a single study of the homoloscleromorph sponge *Oscarella pearsei*  
15 [previously called *O. carmela* (Ereskovsky, et al. unpublished data)] detected the interaction  
16 between  $\beta$ -catenin and a classical cadherin by yeast two-hybrid screen (Nichols, et al. 2012).

17  
18 In general, hypotheses about early animal evolution rest heavily on assumptions made about  
19 developmental regulatory genes in organisms where their function and interactions have been  
20 insufficiently tested. In the case of  $\beta$ -catenin, reported gene expression patterns may reflect the  
21 conservation of one or more bilaterian functions, or entirely alternative functions; it is not  
22 possible to distinguish between these possibilities from *in situ* hybridization data alone.  
23 Likewise, phenotypes produced by pharmacological inhibition of GSK3 $\beta$  may or may not reflect  
24 perturbations to the Wnt/ $\beta$ -catenin pathway; GSK3 $\beta$  is pleiotropic, and  $\beta$ -catenin is not a  
25 confirmed GSK3 $\beta$  substrate in sponges. Here, we examine  $\beta$ -catenin function in the freshwater  
26 sponge, *E. muelleri*. Using an antibody raised against *E. muelleri*  $\beta$ -catenin (Em $\beta$ catenin), we 1)  
27 identify endogenous Em $\beta$ catenin binding partners, 2) characterize tissue-specific Em $\beta$ catenin  
28 populations at the cell membrane (adhesion), the nucleus (signaling), and at probable focal  
29 adhesions in the attachment epithelium (novel function), and 3) find that Em $\beta$ catenin is a  
30 probable substrate of GSK3 $\beta$ .

31  
32  
33  
34

## 1 RESULTS

### 2 Adherens Junction (AJ) and Wnt pathway components in the *E. muelleri* transcriptome

3 We searched the published *E. muelleri* transcriptome (Peña, et al. 2016) and detected a single  
4 ortholog of  $\beta$ -catenin. The *Em $\beta$ catenin* transcript has a predicted 2,685 bp coding sequence,  
5 corresponding to an 895aa predicted peptide. Furthermore, as reported from multiple other  
6 sponge species (Nichols, et al. 2006; Adamska, et al. 2010; Fahey and Degnan 2010; Leininger,  
7 et al. 2014; Riesgo, et al. 2014), we detected conserved homologs of AJ and Wnt signaling  
8 pathway components (Supplement Table S1).

9  
10 *Em $\beta$ catenin* has 53% sequence identity to mouse  $\beta$ -catenin, 50% identity to fly, and between  
11 30-93% identity with  $\beta$ -catenin from other sponge species. The core of the *Em $\beta$ catenin* protein  
12 contains 12 predicted armadillo (Arm) repeats flanked by less conserved and presumably  
13 unstructured N- and C-terminal regions. In bilaterians, the Arm repeat region is known to serve  
14 as the binding interface for interacting with APC, Axin and TCF/Lef which are involved in the  
15 Wnt signaling pathway, but also classical cadherins, a component of AJs (Valenta, et al. 2012).  
16 By aligning *Em $\beta$ catenin* to structurally and functionally characterized orthologs in bilaterians, we  
17 found the conservation of residues Lys-312 and Lys-435 which are required for binding of  
18 mouse  $\beta$ -catenin to E-cadherin (Huber and Weis 2001) (see Fig1 and Supplement Fig S1). Also,  
19 *Em $\beta$ catenin* has conserved GSK3 $\beta$  phosphorylation sites in the N-terminal domain (Ser33,37  
20 and Thr41 in mouse), which are required for initiating the “destruction complex” in the Wnt  
21 signaling pathway (see Fig1 and Supplement Fig S1). The putative binding site for  $\alpha$ -catenin (a  
22 constitutive AJ component) in the N-terminal domain was found to be conserved to a lesser  
23 extent (35% sequence identity with mouse) and only 2 of 5 important binding residues (Miller, et  
24 al. 2013) were conserved in *Em $\beta$ catenin* (Supplement Fig S1).

### 26 Immunoprecipitation (IP) to identify endogenous *Em $\beta$ catenin* binding partners

27 To identify endogenous *Em $\beta$ catenin* binding-partners, we raised an antibody against a 24 kDa  
28 recombinant protein corresponding to the N-terminal region. The resulting antibody was affinity  
29 purified and its specificity tested by Western Blot against whole-cell lysates; a ~110 kDa band  
30 was detected (lower MW bands were also detected, but were lower intensity and therefore  
31 interpreted as probable degradation products) (Fig 2A).

32  
33 To further validate the antibody we performed IP (Fig 2B) coupled with mass spectrometry to  
34 confirm specificity to *Em $\beta$ catenin* and to detect endogenous protein interactions. As

1 summarized in Table 1 (full results available in Supplement), the most abundantly detected  
2 peptides in the precipitate corresponded to Em $\beta$ catenin. Two co-precipitates were  $\alpha$ -catenin  
3 (Em $\alpha$ -catenin) and a classical cadherin (EmCDH2, see (Peña, et al. 2016)); both are homologs  
4 of AJ components. Another co-precipitate was coiled-coil domain-containing protein 91 (ccdc91,  
5 also known as p56). The only available studies of this protein in animals reveal that it is a trans-  
6 Golgi accessory protein involved in vesicle transport between the Golgi and the lysosome  
7 (Mardones, et al. 2007). There is no precedent in the literature for interactions between ccdc91  
8 and  $\beta$ -catenin.

9  
10 We found no evidence for conserved interactions with Wnt pathway components, such as  
11 TCF/Lef, Axin or APC. However, the antibody appeared to be inefficient for use in IP  
12 experiments, as we were unable to visualize discrete bands when precipitates were run on an  
13 SDS-PAGE gel and analyzed by coomassie staining.  $\beta$ -catenin itself could only be detected  
14 within the precipitate by Western blotting (Fig 2B) or mass spectrometry. Furthermore, our  
15 experiments were conducted exclusively on somatic tissues from juvenile sponges, whereas,  
16 Wnt/ $\beta$ -catenin signaling plays an important role in embryonic patterning, and there is evidence  
17 that components of this signaling pathway are developmentally expressed in sponges  
18 (Adamska, et al. 2010; Leininger, et al. 2014). The relationship between genetic mechanisms  
19 that regulate development from a zygote versus development from a gemmule are unknown.

## 21 **Immunostaining to test for adhesion (cell boundary) versus signaling (nuclear)**

### 22 **Em $\beta$ catenin populations**

23 The apical endopinacoderm (AEP) is an epithelium cored by tracts of F-actin that form dense  
24 plaques at points of alignment between neighboring cells (Elliot and Leys, 2007). It has been  
25 proposed that these F-actin plaques resemble desmosomes (but they are more likely AJs, as  
26 desmosomes are phylogenetically restricted to vertebrates). By immunostaining with the  
27 validated  $\beta$ -catenin antibody, we found that Em $\beta$ catenin indeed co-localizes with F-actin  
28 plaques in the AEP (Fig 3). This result is consistent with detected interactions between  
29 Em $\beta$ catenin with Em $\alpha$ -catenin and EmCDH2, and indicates a conserved role for cadherin-  
30 mediated cell-cell adhesion within the AEP.

31  
32 In the attachment epithelium - a cellular monolayer at the interface with the substrate - we  
33 detected continuous cell-boundary staining of Em $\beta$ catenin, consistent with the presence of belt-  
34 AJs. Albeit, this staining was relatively low intensity (see Fig 4). More intense Em $\beta$ catenin

1 staining was evident in the cytosol, at the ends of F-actin stress fibers that closely resemble  
2 Focal Adhesions (FAs) (see Fig4). These stress fibers differ from actin tracts of the AEP in that  
3 they were not regularly oriented in the cell, they were not aligned between neighboring cells,  
4 and did not extend to the full diameter of any individual cell. This result is surprising, because  
5 FAs are integrin-based junctions that mediate interactions between the cell and the extracellular  
6 matrix (ECM). At this point, it is not possible to test for homology to FAs, but this Em $\beta$ catenin  
7 population is not associated with cell-cell contacts, and almost certainly corresponds to cell-  
8 substrate contacts. We might also expect to find FA-like structures in highly migratory cells of  
9 the mesohyl, such as archeocytes. However, we find no evidence for FA-like actin populations  
10 in archeocytes, nor are there filopodia-associated Em $\beta$ catenin populations in these cells (Fig 5).  
11 Solitary cell migration may involve different mechanisms than collective cell migration.

12  
13 Another distinctive, polarized epithelium in sponges is the choanoderm, which consists of  
14 spherical chambers lined with collar cells (i.e. choanocytes), which have an apical ring of  
15 microvilli that surround a central flagellum. These cells pump water through internal canals and  
16 phagocytose bacterial prey. As in the attachment epithelium, in newly developing choanocyte  
17 chambers (see Fig 6A), we detected continuous cell boundary staining of Em $\beta$ catenin.  
18 However, in mature choanocyte chambers (see Fig 6B and C), this staining pattern was less  
19 evident, and instead Em $\beta$ catenin was enriched at points of contact between three adjacent cells  
20 (Fig 6C).

21  
22 Whereas we did not find evidence of conserved interactions between Em $\beta$ catenin and other  
23 Wnt pathway component by IP, we further examined the possible signaling roles of Em $\beta$ catenin  
24 by immunostaining to test for nuclear populations. We detected nuclear Em $\beta$ catenin in the  
25 attachment epithelium (see Fig 7) as well as in migratory cells in the mesohyl (see Fig 5), which  
26 is consistent with a conserved role for Em $\beta$ catenin as a transcriptional coactivator of TCF/Lef.  
27 We did not detect nuclear Em $\beta$ catenin in choanocytes (see Fig 6).

## 28 29 **Is Em $\beta$ catenin a conserved substrate of GSK3 $\beta$ ?**

30 GSK3 $\beta$  is a negative regulator of  $\beta$ -catenin in the Wnt/ $\beta$ -catenin signaling pathway, and  
31 previous studies have shown that treating sponges with multiple, independent GSK3 $\beta$  inhibitors  
32 has reproducible phenotypic effects. To more directly test whether the effects of GSK3 $\beta$  are  
33 related to Wnt/ $\beta$ -catenin signaling, we sought to examine whether GSK3 $\beta$  inhibitors affect  
34 endogenous Em $\beta$ catenin phosphorylation states. We treated juvenile *E. muelleri* sponges with



1 the GSK3 $\beta$  inhibitors Alsterpaullone and BIO, and monitored their effects by Western Blot (see  
2 Fig 8). We detected an increase in electrophoretic mobility of Em $\beta$ catenin in lysates from  
3 GSK3 $\beta$  inhibited sponges, which we interpreted as a change in the Em $\beta$ catenin phosphorylation  
4 state (dephosphorylated Em $\beta$ catenin was expected to migrate faster in the gel). As  
5 confirmation, the electrophoretic migration rate of Em $\beta$ catenin was also monitored in sponge  
6 lysates that were variously treated with phosphatases, phosphatase inhibitors, both, or neither.  
7 We found that phosphatase treatment increased the electrophoretic mobility of Em $\beta$ catenin,  
8 whereas phosphatase inhibition decreased electrophoretic mobility (Supplement Fig S3).

9  
10 Through titration of the GSK3 $\beta$  inhibitors we determined that treatment with ~ 0.1  $\mu$ M AP or ~1  
11  $\mu$ M BIO resulted in a complete shift from phosphorylated to dephosphorylated states of  
12 Em $\beta$ catenin and was therefore considered the minimal effective dosage (Fig 8). Sponges  
13 treated with this dosage lacked canals and the choanoderm was either absent or malformed.  
14 Thus, GSK3 $\beta$  inhibition at the minimal effective dosage disrupts the development of the  
15 aquiferous system, including differentiation of the choanoderm (Fig 9).

16  
17 Efforts were also made to directly disrupt Em $\beta$ catenin function using RNAi and Vivo-  
18 morpholinos. These techniques caused non-specific phenotypic effects (which varied between  
19 individuals collected from different localities), but no measurable change in Em $\beta$ catenin levels  
20 as measured by Western Blot (Supplement Fig S4).

## 21 22 **DISCUSSION**

23  $\beta$ -catenin is thought to have played a critical role in animal body plan evolution due to its  
24 pleiotropic roles in development signaling (Wnt signaling pathway) and in cadherin-based cell-  
25 cell adhesion. These roles are broadly conserved in all studied animals, but functional data are  
26 available from only cnidarians and bilaterians. Earlier diverging animal lineages -- including  
27 sponges -- have conserved homologs of Wnt pathway and cell adhesion genes, but there is  
28 limited experimental evidence pertaining to their function. Thus, hypotheses about the role of  
29 Wnt signaling and cadherin-based cell adhesion during the earliest periods of animal evolution  
30 depend partly upon improved understanding of  $\beta$ -catenin function in these understudied  
31 lineages.

32  
33 Looking outside of animals, there is evidence for a possible  $\beta$ -catenin homolog (*Aardvark*) in the  
34 social amoeba *Dictyostelium discoideum* that interacts with an  $\alpha$ -catenin-like protein to regulate

1 the polarity of the tip epithelium of the fruiting body (Dickinson, et al. 2011). Nevertheless, *D.*  
2 *discoideum* lacks both cadherins and Wnt pathway components. If we consider lineages that  
3 are more closely related to animals, cadherins have been detected in several unicellular  
4 opisthokonts, but they lack  $\beta$ -catenin interacting regions, they lack conserved  $\beta$ -catenin  
5 orthologs, and there is no evidence for other conserved Wnt pathway components (Abedin and  
6 King 2008; Nichols, et al. 2012). Collectively, these data suggest that the pleiotropic functions of  
7  $\beta$ -catenin in cell adhesion and Wnt signaling are an early innovation in the animal stem lineage.

8

### 9 **Adherens junctions (AJs) in sponges**

10 The presence of AJs has been predicted in sponges based upon genome and transcriptome  
11 data from diverse species (Nichols, et al. 2006; Srivastava, et al. 2010; Nichols, et al. 2012;  
12 Riesgo, et al. 2014), and upon limited ultrastructural evidence [reviewed in (Leys, et al. 2009)].  
13 Our Em $\beta$ catenin Co-IP data provide new experimental support for endogenous interactions  
14 between AJ components in *E. muelleri*. Notably, we detected an interaction between  
15 Em $\beta$ catenin with EmCDH2 and Em $\alpha$ -catenin, even though the residues required for the latter  
16 interaction are incompletely conserved in *E. muelleri* (Miller, et al. 2013). This result  
17 underscores the limitations of functional predictions made using exclusively bioinformatic  
18 approaches, and parallels the example of Axin in the sponge *O. pearsei*, which lacks the  
19 expected binding motif for  $\beta$ -catenin but was identified as a binding partner via yeast two-hybrid  
20 screen (Nichols, et al. 2012). A possible explanation for why EmCDH2 and not EmCDH1 was  
21 detected as a candidate Em $\beta$ catenin binding partner is that EmCDH1 may be expressed at a  
22 different developmental stage than the juvenile tissues examined. In bilaterians, classical  
23 cadherins often exhibit tissue-specific expression. For example, E-cadherin is  
24 expressed in epithelial tissues, N-cadherin expressed in the nervous system, and P-cadherin in  
25 the placenta. As sponges appear to be largely epithelial organisms it is intriguing to consider  
26 that they may have different adhesion receptors expressed in different contexts. Spatiotemporal  
27 differences in expression of cadherin paralogs may reveal differences in the evolutionary history  
28 and organization of different sponge tissues.

29

30 Immunostaining of Em $\beta$ catenin further supports the existence of AJs in sponge tissues.  
31 Continuous cell boundary staining is evident in the attachment epithelium (Fig 4) as well as in  
32 newly developing choanocyte chambers (Fig 6A). This staining pattern resembles the  
33 organization of AJs in cnidarian and bilaterian epithelial tissues, which form a continuous ‘belt’  
34 around the periphery of the cell, thereby dividing the plasma membrane into apical and

1 basolateral domains. Together with occluding junctions (tight junctions in vertebrates and  
2 septate junctions in invertebrates), AJs can help create a barrier that regulates paracellular  
3 transport, effectively separating the environment outside of the tissue from the interior  
4 environment -- a fundamental feature of multicellular organization (Banerjee, et al. 2006;  
5 Hartsock and Nelson 2008; Zihni, et al. 2016). There is evidence that freshwater sponges have  
6 “sealed” epithelia (Adams, et al. 2010), but it is not yet established which molecules are  
7 involved.

8  
9 Instead of continuous cell-boundary staining, mature choanoderm tissue (Fig 6C) and the AEP  
10 (Fig 3) were found to have probable adhesion-associated Em $\beta$ catenin populations with a much  
11 more restricted distribution. In mature choanocyte chambers, Em $\beta$ catenin was largely enriched  
12 at lateral membranes where three adjacent cells adjoin; this localization pattern superficially  
13 resembles tricellular junctions of *Drosophila*, although they have a different molecular  
14 composition than AJs. In the AEP, Em $\beta$ catenin co-localizes with F-actin plaques that form  
15 where F-actin stress fibers are aligned between neighboring cells. This is consistent with the  
16 view that the AEP is a contractile epithelium (Elliott and Leys 2007; Nickel, et al. 2011) and that  
17 the plaques represent AJs that form at focal points of tissue stress.

### 18 19 **A possibly novel cell-substrate adhesion role for Em $\beta$ catenin**

20 Detected interactions of Em $\beta$ catenin with Em $\alpha$ -catenin and EmCDH2, and its presence at cell-  
21 cell contacts, support predictions about its possible role in AJs in sponge tissues. A less  
22 expected result is the detection of Em $\beta$ catenin at FA-like structures in the attachment epithelium  
23 (Fig 4). FAs are well-characterized cell junctions that utilize integrins rather than cadherins as  
24 adhesion receptors to mediate interactions between cells and the ECM. Despite this staining  
25 pattern, we found no evidence that FA components co-precipitate with Em $\beta$ catenin, and in  
26 bilaterians  $\beta$ -catenin is not a typical FA component. However, Langhe and colleagues (2016)  
27 have shown that *Xenopus*  $\beta$ -catenin and cadherin 11 co-localize with FA components when  
28 overexpressed in HeLa cells and Kuo and colleagues (2011) found  $\beta$ -catenin associated with  
29 FAs isolated from HFF1 cells. The functional significance of these studies is unknown, and thus  
30 the implications for our finding of Em $\beta$ catenin at FA-like structures in *E. muelleri* is unclear.

31  
32 It is possible that classical cadherins mediate both cell-cell and cell-matrix adhesion in *E.*  
33 *muelleri*. Like classical cadherins in *Drosophila* and other non-chordate animals, EmCDH1 and  
34 EmCDH2 have membrane-proximal epithelial growth factor (EGF) and Laminin G (LamG)

1 domains (Supplement Fig S2). In *Drosophila* this region has been implicated in trafficking to the  
2 plasma membrane (Oda and Tsukita 1999), but in an unusual classical cadherin-like protein  
3 (BbC) in the lancelet *Branchiostoma*, this region is sufficient to mediate epithelial cell adhesion  
4 (BbC naturally lacks cadherin repeats; (Oda, et al. 2002; Oda, et al. 2004)). In general, EGF and  
5 LamG are involved in extracellular protein interactions and are common in both cell surface  
6 receptors and secreted components of the ECM. In the future, it will be critical to determine the  
7 expression dynamics and subcellular localization of candidate sponge adhesion receptors,  
8 themselves; both integrins and classical cadherins.

9

### 10 **Evidence for a functional Wnt/ $\beta$ -catenin pathway in sponges**

11 Activation of the Wnt/  $\beta$ -catenin signaling pathway results in the stabilization of cytosolic  $\beta$ -  
12 catenin and its subsequent translocation to the nucleus. In *E. muelleri*, we find no evidence for  
13 conserved interactions of Em $\beta$ catenin with Wnt pathway components (such as TCF/Lef, Axin or  
14 APC) by Co-IP, but by immunostaining we detect a nuclear population of Em $\beta$ catenin in cells of  
15 the attachment epithelium and in archeocytes (migratory cells within of the mesohyl) where it  
16 presumably functions as a transcriptional coactivator. Additionally, we find evidence that  
17 Em $\beta$ catenin is a substrate of GSK3 $\beta$  in *E. muelleri*, as inhibition of GSK3 $\beta$  leads to a shift in  
18 endogenous Em $\beta$ catenin phosphorylation states. This resembles the condition in bilaterians,  
19 where GSK3 $\beta$  functions as a negative regulator of Wnt signaling by phosphorylating free  
20 cytosolic  $\beta$ -catenin, leading to its ubiquitination and degradation via the proteasome.

21

22 Archeocytes are hypothesized to be pluripotent cells. Part of the evidence for this perspective is  
23 that they express stem cell markers such as *Musashi* and *Piwi* (Alié, et al. 2015), and disruption  
24 of archeocyte cell division inhibits differentiation of the choanoderm (Peña, et al. 2016). Thus,  
25 detection of nuclear Em $\beta$ catenin in archeocytes is consistent with the known role of Wnt/ $\beta$ -  
26 catenin signaling in bilaterian stem-cell maintenance and renewal. Wnt/ $\beta$ -catenin pathway  
27 genes expression has also been reported in archeocytes of the sponges *A. queenslandica*  
28 (Adamska, et al. 2010) and *S. ciliatum* (Leininger, et al. 2014). If  $\beta$ -catenin has a conserved role  
29 in maintaining archeocyte pluripotency in *E. muelleri*, it may explain aspects of the aquiferous  
30 system phenotypes observed with GSK3 $\beta$  inhibition. Specifically, sustained activation of the  
31 Wnt/ $\beta$ -catenin pathway may inhibit differentiation of archeocytes into choanocytes.

32

33 A nuclear population of Em $\beta$ catenin is also present in cells of the attachment epithelium. One  
34 possible explanation of this finding comes from a study implicating Wnt/ $\beta$ -catenin signaling as

1 an upstream regulator of collective cell migration in the migrating zebrafish lateral line  
2 primordium, particularly in cells of the leading edge of migration (Aman and Piotrowski 2008). It  
3 is well established that sponges are capable of entire-colony mobility, and in juveniles of *E.*  
4 *muelleri* this behavior is the result of collective migration of the attachment epithelium (Bond and  
5 Harris 1988; Bond 1992). Furthermore, FAs are well-known to be dynamically regulated during  
6 bilaterian cell migration (particularly when migrating on a 2D surface), and FA-like structures are  
7 present in the attachment epithelium (Sastry and Burrridge 2000; Stehbens and Wittmann 2012;  
8 Kim and Wirtz 2013).

9  
10 A limitation of our study is that we were restricted to working with gemmule-hatched juvenile  
11 tissues, whereas Wnt/ $\beta$ -catenin has previously been implicated in embryonic development in  
12 other sponge species. Specifically, in *A. queenslandica* (Adamska, et al. 2010) and *S. ciliatum*  
13 (Leininger, et al. 2014), Wnt/ $\beta$ -catenin pathway genes were found to exhibit posterior/anterior  
14 expression gradients during embryogenesis, consistent with a conserved role in axial patterning.  
15 These data are difficult to relate to our findings in *E. muelleri* because embryogenesis is a  
16 fundamentally different process than gemmule hatching, and the regulatory similarities between  
17 these disparate developmental processes have never been examined. Nonetheless, Windsor  
18 and Leys (Windsor and Leys 2010) also studied gemmule-hatched *E. muelleri* juveniles and  
19 reported that GSK3 $\beta$  inhibition disrupted development of the aquiferous system and caused the  
20 formation of ectopic oscula. From these data, they hypothesized that the adult body axis in  
21 sponges may be defined by the unidirectional aquiferous system. Whereas our data do not bear  
22 on this question directly, they do support the underlying assumption that Em $\beta$ catenin is a  
23 substrate of GSK3 $\beta$  in *E. muelleri*, and confirm that the minimal effective dosages of GSK3 $\beta$   
24 inhibition of  $\beta$ -catenin phosphorylation recapitulate the reported knockdown phenotypes.

25  
26 Finally, a gene expression study in *S. ciliatum* has also implicated Wnt/ $\beta$ -catenin signaling in  
27 endomesoderm specification, and revealed  $\beta$ -catenin expression in the embryonic micromeres  
28 (precursors of choanocytes) as well as mature choanocytes and mesohyl cells (Leininger, et al.  
29 2014). Based upon this study, it was hypothesized that sponges have germ layers homologous  
30 to those of bilaterians and that the choanoderm derives from endoderm. However, contradictory  
31 data from lineage-tracing experiments in *A. queenslandica* indicate that cell layers in sponges  
32 do not undergo progressive fate determination and are therefore not homologous to  
33 bilaterian germ layers (Nakanishi, et al. 2014). Our data bear on this question only in that we  
34 detect a cell-adhesion-associated population of Em $\beta$ catenin in the choanoderm, but not a

1 nuclear population. It is therefore possible that the  $\beta$ -catenin expression detected in the  
2 choanoderm of *S. ciliatum* relates to its roles in cell adhesion in this tissue rather than Wnt  
3 signaling. However, it is notable that the modern sponge lineages to which *E. muelleri* and *S.*  
4 *ciliatum* belong, diverged ~750-850 Ma, during the Neoproterozoic (Dohrmann and Wörheide  
5 2017), and they have quite divergent developmental features. Furthermore, Wnt pathway  
6 components other than  $\beta$ -catenin are also expressed in the choanoderm of *S. ciliatum*.

7

## 8 **SUMMARY AND CONCLUSIONS**

9 Here, we study  $\beta$ -catenin in the freshwater sponge *E. muelleri* and find 1) that AJ components  
10 ( $\alpha$ -catenin and classical cadherin), but no Wnt pathway components, co-precipitate with  
11 endogenous Em $\beta$ catenin from whole-cell lysates, 2) there are cell boundary (adhesion-related)  
12 and nuclear (signaling-related) populations of Em $\beta$ catenin, 3) that previously reported  
13 phenotypic effects of GSK3 $\beta$  inhibitors on aquiferous system development can be replicated  
14 and are associated with shifts in Em $\beta$ catenin phosphorylation state, and 4) there is an  
15 Em $\beta$ catenin population associated with FA-like structures in the attachment epithelium,  
16 reflecting a potentially novel function.

17

18 The evidence presented here supports the underlying assumptions of previous studies: that  $\beta$ -  
19 catenin has conserved functions in Wnt signaling and cadherin-based cell adhesion in sponges.  
20 However, the discovery of a  $\beta$ -catenin population associated with FA-like, cell-substrate  
21 adhesion structures underscores that functional conservation should not be uncritically accepted  
22 based upon bioinformatics and gene expression studies alone. Particularly, in the case of  
23 pleiotropic genes, the interpretation of gene expression patterns is potentially fraught without  
24 more explicit functional and biochemical support. To this end, future progress will depend  
25 largely upon the development of experimental approaches to manipulate gene function directly,  
26 *in vivo*, without the ambiguities that accompany pharmacological approaches. Moreover,  
27 comparative research should continue in multiple sponge species, as modern sponges  
28 represent many anciently divergent lineages.

29

30

31

32

33

34

## 1 MATERIAL AND METHODS

### 2 Collection and growing of sponges

3 Adult specimens of *E. muelleri* containing gemmules were collected in October 2013 from upper  
4 Red Rock Lake, Colorado, USA. The gemmule-bearing sponges were stored in autoclaved lake  
5 water in the dark at 4 °C and water was periodically refreshed. Gemmules were removed from  
6 the adult by gentle rubbing of the sponge tissue or by picking gemmules from the tissue with  
7 forceps. To clean the gemmules, they were washed several times with autoclaved lakewater.

8

9 For obtaining sponge cell lysate for Co-IP, ~100 sponges were cultivated in a petridish (90 mm  
10 diameter) containing 25 ml of autoclaved lake water or sterile M-medium (1 mM CaCl<sub>2</sub>·6H<sub>2</sub>O,  
11 0.5 mM MgSO<sub>4</sub>·7H<sub>2</sub>O, 0.5 mM NaHCO<sub>3</sub>, 0.05 mM KCl, 0.25 mM Na<sub>2</sub>SiO<sub>3</sub>; (Funayama, et al.  
12 2005)) in the dark at room temperature (20-22 °C). Typically sponges hatched 4-5 days after  
13 plating. After hatching, the lakewater or M-medium was refreshed every other day. Three to four  
14 days after hatching the sponges were fully developed and were harvested to make cell lysates.

15

16 To culture sponges for immunostaining and the pharmacological studies, #1.5 22mmx22mm  
17 glass coverslips were placed into 6-well plate format and each well would contain 5 ml of  
18 autoclaved lakewater or M-medium. The individual gemmules were placed on the coverslips in  
19 the dark at room temperature (20-22 °C). Again, 3-4 days after hatching the sponges were fixed  
20 for immunostaining or harvested for western blot analysis.

21

### 22 cDNA library construction

23 Material for constructing the cDNA library was obtained from juvenile sponges that had  
24 developed from hatched gemmules. All gemmules were collected from one adult specimen of *E.*  
25 *muelleri*. Total RNA (~ 1 mg) was isolated using TRIzol Reagent (ThermoFischer Scientific  
26 #15596026) following manufacturer's instructions. To purify mRNA from total RNA we used  
27 Oligotex Suspension (Qiagen #79000) and followed the protocol "Purification of Poly A+ mRNA  
28 from Total RNA using a Batch Procedure" from the Oligotex handbook (pg. 23-25). The purified  
29 mRNA was then concentrated using Corning Spin-X UF 500 µl Concentrators with a molecular  
30 weight cut-off of 10,000 (Corning #431478). To construct the cDNA library we used the  
31 CloneMiner II cDNA Library Construction Kit (ThermoFischer Scientific #A11180) according to  
32 the manufacturer's instructions.

33

34

## 1 **Protein expression and purification**

2 The N-terminal part of *E. muelleri*  $\beta$ -catenin (Em $\beta$ catN amino acids 1-221) was amplified by  
3 PCR from *E.muelleri* cDNA with the following primers:

4  
5 Em $\beta$ catN forward:

6 1) tacttccaatccaatgcaATGGAGGTGGACAGATCATACTAC, which contains an LIC adapter  
7 (lower case)

8 Em $\beta$ catN reverse

9 2) ttatccactccaatgttattaCTAGAGCTCGGAGGAACCCTGAT, which contains an LIC adapter  
10 (lower case) and a STOP codon (underlined).

11  
12 The amplified fragment was cloned into the pET His6 Sumo TEV LIC cloning vector (1S)  
13 (Addgene plasmid # 29659). This vector generates proteins that are N-terminally tagged with a  
14 TEV-cleavable His6-Sumo fusion tag. The construct was transformed into *Escherichia coli*  
15 Rosetta (DE3) competent cells (Novagen). Recombinant protein expression was induced at  
16 OD600 ~0.4 and was conducted at room temperature for 6 hours (0.25 mM IPTG). Cells were  
17 spun down and resuspended in cell resuspension buffer (1x PBS, 2M NaCl, 5% glycerol, 0.1  
18 mM PMSF, pH 8.0) with lysozyme (1mg/ml) and incubated at room temperature for 10 min.  
19 Cells were sonicated by 4 x 30sec pulses and bacterial debris was removed by centrifugation at  
20 20,000xg for 30 min at 4 °C. To purify the recombinant protein, the supernatant was incubated  
21 with HisPur Cobalt Resin (ThermoFisher # 89964) overnight at 4 °C. The beads were washed  
22 with washing buffer (1xPBS, 5% glycerol, pH 8.0) and the His-tagged proteins were eluted with  
23 elution buffer (150 mM imidazole, 1 x PBS, 5% glycerol, pH 8.0). To cleave the His6-Sumo  
24 fusion tag, recombinant proteins were incubated with AcTEV protease (ThermoFischer #  
25 12575015) overnight at 4 °C, using 1 U for ~40  $\mu$ g of recombinant protein. To remove imidazole  
26 and DTT, a buffer exchange was performed using PD-10 Desalting columns (GE Healthcare #  
27 17-0851-01) and the protein samples were equilibrated in 1x PBS (pH 8.0) with 5% glycerol.  
28 Subsequently HisPur Cobalt resin was used to remove the His6-Sumo tag and AcTEV protease.  
29 The eluate contained the Em $\beta$ catN recombinant protein (without His6-Sumo fusion tag), which  
30 was used to inject in rabbits.

31

## 32 **Antibody Production**

33 Polyclonal antibodies were raised in rabbits against recombinant Em $\beta$ catN antigen (Syd labs,  
34 Natick, USA) and the anti-Em $\beta$ catN antibodies were affinity purified from the rabbit serum using



1 recombinant Em $\beta$ catN protein with the AminoLink Plus Immobilization Kit (ThermoFischer,  
2 #44894) according to the manufacturer's instructions. Two Amino-link resin columns were  
3 prepared, one with Em $\beta$ catN recombinant protein and one with *E. coli* proteins. First the rabbit  
4 serum was incubated with the *E.coli* protein-column by running it 10x over the column to remove  
5 possible IgG's against bacterial proteins. Next, the eluate was incubated with the Em $\beta$ catN  
6 protein-column by running it 10x over the column and the column was washed extensively with  
7 1x PBS. Finally, the affinity-purified antibody was eluted from the column with Elution buffer (0.1  
8 M Glycine, pH 2.5) and neutralized with Neutralization buffer (0.75M Tris, pH 8.8). The fractions  
9 with the highest amount of antibodies were combined, and buffer was exchanged with PD-10  
10 Desalting columns and the affinity purified antibody was equilibrated in 1x PBS with 0.05%  
11 sodium azide. The final concentration of antibody was ~ 1 mg/ml.

12

### 13 **Co-IP and Mass Spectrometry**

14 Two independent Em $\beta$ catenin Co-IP experiments were performed using Dynabeads Protein G  
15 for Immunoprecipitation (ThermoFischer Scientific, # 10004D) according to the manufacturer's  
16 instructions. For each experiment, we coupled 5  $\mu$ g of Em $\beta$ catN-antibody to 50  $\mu$ l (=1.5 mg) of  
17 Dynabeads protein G. As a negative we control, we also coupled normal rabbit IgG (Santa Cruz  
18 Biotechnology, #sc-2027) to Dynabeads. To crosslink the antibody to the beads, the antibody-  
19 coupled beads were incubated with 350  $\mu$ l of 0.75 mM BS3 crosslinker (ThermoFischer  
20 Scientific, #21580) in conjugation buffer (20mM Sodium Phosphate, 0.15M NaCl, pH 8.1) for 30  
21 min at room temperature, crosslinking reaction was stopped by adding 17.5  $\mu$ l Quenching buffer  
22 (1M Tris-HCl, pH 7.5), and the beads were washed with PBST (0.1% Tween-20).

23

24 Whole cell lysates were derived from ~1 week old gemmule-hatched juveniles. At this stage, all  
25 somatic tissues had developed. The lysate was prepared by dissolving the juvenile sponges in  
26 lysis buffer (20 mM Hepes, pH 7.6, 150 mM NaCl, 1 mM EDTA, 10% Glycerol, 1% Triton X-100,  
27 1 mM DTT, 1 mM PMSF, 1x phosphatase inhibitor cocktail A and B (Biotool, #B15001), 1x  
28 protease inhibitor cocktail (Biotool, #B14011, EDTA free)). The crude lysate was clarified by  
29 centrifugation at 14,000xg for 10min at 4 °C. From the crude lysate we took 600  $\mu$ g of soluble  
30 sponge proteins (measured with Bradford Protein Assay) and diluted this 2x with  
31 binding/washing buffer (same as lysis buffer, but without glycerol and DTT). The lysate was  
32 incubated with the antibody-coupled beads for 1.5 hr at 4 °C, and was washed with  
33 binding/washing buffer and proteins were eluted with 50  $\mu$ l of 0.2 M Glycine pH 2.5.

34

1 The samples were digested, desalted and analyzed with mass spectrometry by EPFL-  
2 Plateforme technologique de proteomique using Orbitrap Elite (4x short LC-MS/MS gradient).  
3 The raw data was searched against the *E. muelleri* protein database using Scaffold software  
4 with a protein threshold of 99% and a peptide threshold of 95%. We compared the results with  
5 the control IP (rabbit IgG) to identify non-specific interactions of sponge proteins with IgG-  
6 coupled Dynabeads. We selected proteins that had at least 5 unique peptide matches and no  
7 hits in the control-IP (see Table 1. For a complete list of all identified proteins, see Supplement  
8 Table S2).

9

## 10 **Immunostaining**

11 Sponges that grew on the coverslips in 6-wells format plates were fixed with ice-cold EtOH with  
12 4% formaldehyde for 1 h at 4 °C. To remove the fixative, the sponges were washed 3x with  
13 PBST (0.1% Tween-20). The coverslips containing the coverslips were transferred to parafilm in  
14 a humid chamber. First sponges were incubated with blocking reagent (3% BSA in PBST (0.1%  
15 Tween-20)) for 1 h at room temperature. Next, they were incubated with the primary antibody  
16 (anti-Em $\beta$ catN 1:500 in blocking reagent) for 2 hrs at room temperature or overnight at 4 °C.  
17 After incubating with the primary antibody, sponges were washed 3x with PBST and were  
18 incubated with the secondary antibody (1:300, goat anti-rabbit Alexa Fluor 488, ThermoFischer  
19 #A11034) together with Alexa Fluor 568 Phalloidin (1:40, ThermoFischer #A12380) and  
20 Hoechst33342 (1  $\mu$ g/ml) in blocking reagent for 45 min at room temperature. Sponges were  
21 washed 3x with PBS before they were mounted with mounting medium (90% glycerol, 1x PBS,  
22 0.1 M propyl gallate) on a microscopic glass slide with clay feet and sealed into place with  
23 heated VALAP (vaseline, lanolin and paraffin, 1:1:1). The negative controls were incubated with  
24 secondary antibody only. Images were taken with a 60x and 100x oil immersion objective on an  
25 Olympus Fluoview 1000 inverted confocal microscope, and images were processed using  
26 ImageJ (z-stack: maximal intensity projection).

27

## 28 **Pharmacological treatment (AP and BIO) and Western blot analysis**

29 All treatments were done in sterile M-medium with different concentrations of AP  
30 (Alsterpaullone, Sigma-Aldrich #A4847) and BIO (6-bromoindirubin-3'-oxime, Sigma-Aldrich  
31 #B1686). The tested concentrations for AP were 0.025  $\mu$ M, 0.05  $\mu$ M, 0.1  $\mu$ M and 0.2  $\mu$ M and for  
32 BIO 0.125  $\mu$ M, 0.25  $\mu$ M, 0.5  $\mu$ M and 0.1  $\mu$ M. Since AP and BIO were initially dissolved in DMSO  
33 (10 mM stocks), the control treatments consisted of 0.02% DMSO in M-medium. Sponges were  
34 treated for the duration of the experiment and were imaged during day 5, 6 and 7 using a Leica

1 MZ 16FA stereoscope. At day 7, sponges were harvested for Western Blot analysis. To prepare  
2 samples for western blot, sponges were dissolved in 1x Lysis buffer and samples were boiled  
3 together with Laemmli loading buffer for 5 min, followed by a quick spin. The protein samples  
4 (~2 sponges per lane) were separated by SDS-PAGE on an 8% gel and the proteins were  
5 transferred to a PVDF membrane (Bio-Rad #1620177). Membranes were blocked for 1 h at  
6 room temperature in blocking solution (5% non-fat dry milk in 1x PBST (0.1% Tween-20)), and  
7 then incubated with anti-Em $\beta$ catN antibody (1:10.000) in blocking solution overnight at 4 °C  
8 Membranes were washed extensively with PBST and incubated with the secondary antibody  
9 (goat anti-rabbit IgG antibody, horseradish peroxidase conjugate, Promega #W401B 1:5000) in  
10 blocking solution for 1h at room temperature. Again membranes were washed extensively in  
11 PBST and were developed using Western Lightning Plus Enhanced Chemiluminescence  
12 Substrate (PerkinElmer #NEL104001EA). To visualize the loading control, the membrane was  
13 stripped and reprobred. Stripping was done by incubating the membrane for 10 min at room  
14 temperature in mild stripping buffer (1.5% w/v glycine, 0.1% w/v SDS and 0.1% w/v Tween-20)  
15 and washing extensively in PBS and PBST. Reprobing procedure was similar as described  
16 above, but using mouse anti-alpha tubulin (1:10.000, Sigma Aldrich #T5168) as a primary  
17 antibody and goat anti-mouse rabbit IgG antibody, horseradish peroxidase conjugate (1:5000  
18 Promega #W402B) as a secondary antibody.

19

## 20 **ACKNOWLEDGEMENTS**

21 The authors thank Brigitte Galliot for providing labspace, reagents and administrative support;  
22 Detlev Arendt for providing support to finalize the project; and Jennyfer Mora Mitchell for help  
23 with field collection of *E. muelleri*. This work was supported by a Marie-Curie Fellowship (FP7-  
24 PEOPLE-2012-IOF- 327684 Sponge Signaling) to K.J.S. and the University of Denver Faculty  
25 Research Fund to S.A.N.

26

27

28

29

30

31

32

33

34

## REFERENCES

- Abedin M, King N. 2008. The premetazoan ancestry of cadherins. *Science* 319:946-948.
- Adams EDM, Goss GG, Leys SP. 2010. Freshwater sponges have functional, sealing epithelia with high transepithelial resistance and negative transepithelial potential. *PloS one* 5:e15040.
- Adamska M, Larroux C, Adamski M, Green K, Lovas E, Koop D, Richards GS, Zwafink C, Degnan BM. 2010. Structure and expression of conserved Wnt pathway components in the demosponge *Amphimedon queenslandica*. *Evol Dev* 12:494-518.
- Alié A, Hayashi T, Sugimura I, Manuel M, Sugano W, Mano A, Satoh N, Agata K, Funayama N. 2015. The ancestral gene repertoire of animal stem cells. *Proc Natl Acad Sci U S A* 112:E7093-E7100.
- Aman A, Piotrowski T. 2008. Wnt/ $\beta$ -catenin and Fgf signaling control collective cell migration by restricting chemokine receptor expression. *Dev Cell* 15:749-761.
- Banerjee S, Sousa AD, Bhat MA. 2006. Organization and function of septate junctions. *Cell Biochem Biophys* 46:65-77.
- Bond C. 1992. Continuous cell movements rearrange anatomical structures in intact sponges. *J Exp Zool* 263:284-302.
- Bond C, Harris AK. 1988. Locomotion of sponges and its physical mechanism. *J Exp Zool* 246:271-284.
- Capaldo CT, Macara IG. 2007. Depletion of E-cadherin disrupts establishment but not maintenance of cell junctions in madin-darby canine kidney epithelial cells. *Mol Biol Cell* 18:189-200.
- Clarke DN, Miller PW, Lowe CJ, Weis WI, Nelson WJ. 2016. Characterization of the cadherin–catenin complex of the sea anemone *Nematostella vectensis* and implications for the evolution of metazoan cell–cell adhesion. *Mol Biol Evol* 33:2016-2029.
- Clevers H, Nusse R. 2012. Wnt/ $\beta$ -catenin signaling and disease. *Cell* 149:1192-1205.

Dickinson DJ, Nelson WJ, Weis WI. 2011. A polarized epithelium organized by  $\beta$ - and  $\alpha$ -catenin predates cadherin and metazoan origins. *Science* 331:1336-1339.

Dohrmann M, Wörheide G. 2017. Dating early animal evolution using phylogenomic data. *Sci Rep* 7:3599.

Dunn CW, Leys SP, Haddock SHD. 2015. The hidden biology of sponges and ctenophores. *Trends Ecol Evol* 30:282-291.

Elliott GRD, Leys SP. 2007. Coordinated contractions effectively expel water from the aquiferous system of a freshwater sponge. *J Exp Biol* 210:3736-3748.

Ereskovsky A, Richter DJ, Lavrov DV, Schippers KJ, Nichols SA. unpublished data. Transcriptome sequencing and delimitation of cryptic *Oscarella* species (*O. carmela* and *O. pearsei* sp. nov) from California, USA. bioRxiv:doi.org/10.1101/126326.

Fahey B, Degnan BM. 2010. Origin of animal epithelia: insights from the sponge genome. *Evol Dev* 12:601-617.

Fernàndez-Busquets X, Burger MM. 1997. The main protein of the aggregation factor responsible for species-specific cell adhesion in the marine sponge *Microciona prolifera* is highly polymorphic. *J Biol Chem* 272:27839-27847.

Funayama N, Nakatsukasa M, Hayashi T, Agata K. 2005. Isolation of the choanocyte in the fresh water sponge, *Ephydatia fluviatilis* and its lineage marker, *Ef annexin*. *Dev Growth Differ* 47:243-253.

Grice LF, Gauthier MEA, Roper KE, Fernàndez-Busquets X, Degnan SM, Degnan BM. 2017. Origin and evolution of the sponge aggregation factor gene family. *Mol Biol Evol* 34:1083-1099.

Hartsock A, Nelson WJ. 2008. Adherens and tight junctions: Structure, function and connections to the actin cytoskeleton. *Biochim Biophys Acta Biomembranes* 1778:660-669.

Henkart P, Humphreys S, Humphreys T. 1973. Characterization of sponge aggregation factor. A unique proteoglycan complex. *Biochemistry* 12:3045-3050.

Hobmayer B, Rentzsch F, Kuhn K, Happel CM, von Laue CC, Snyder P, Rothbacher U, Holstein TW. 2000. WNT signalling molecules act in axis formation in the diploblastic metazoan *Hydra*. *Nature* 407:186-189.

Holstein TW. 2012. The evolution of the Wnt pathway. *Cold Spring Harb Perspect Biol* 4:a007922.

Huber AH, Weis WI. 2001. The structure of the  $\beta$ -catenin/E-cadherin complex and the molecular basis of diverse ligand recognition by  $\beta$ -catenin. *Cell* 105:391-402.

Jager M, Dayraud C, Mialot A, Quéinnec E, Guyader H, Manuel M. 2013. Evidence for involvement of Wnt signalling in body polarities, cell proliferation, and the neuro-sensory system in an adult ctenophore. *PLoS one* 8:e84363.

Kim D-H, Wirtz D. 2013. Focal adhesion size uniquely predicts cell migration. *FASEB J* 27:1351-1361.

Kuo J-C, Han X, Hsiao C-T, Yates Iii JR, Waterman CM. 2011. Analysis of the myosin-II-responsive focal adhesion proteome reveals a role for  $\beta$ -Pix in negative regulation of focal adhesion maturation. *Nat Cell Biol* 13:383-393.

Kusserow A, Pang K, Sturm C, Hroudá M, Lentfer J, Schmidt HA, Technau U, Haeseler A, Hobmayer B, Martindale MQ, et al. 2005. Unexpected complexity of the Wnt gene family in a sea anemone. *Nature* 433:156-160.

Langhe RP, Gudzenko T, Bachmann M, Becker SF, Gonnermann C, Winter C, Abbruzzese G, Alfandari D, Kratzer M-C, Franz CM, et al. 2016. Cadherin-11 localizes to focal adhesions and promotes cell–substrate adhesion. *Nat Commun* 7:10909.

Lapébie P, Gazave E, Ereskovsky A, Derelle R, Bézac C, Renard E, Houliston E, Borchiellini C. 2009. WNT/ $\beta$ -catenin signalling and epithelial patterning in the homoscleromorph sponge *Oscarella*. *PLoS one* 4:e5823.

Lee PN, Pang K, Matus DQ, Martindale MQ. 2006. A WNT of things to come: Evolution of Wnt signaling and polarity in cnidarians. *Semin Cell Dev Biol* 17:157-167.

Leininger S, Adamski M, Bergum B, Guder C, Liu J, Laplante M, Brate J, Hoffmann F, Fortunato S, Jordal S, et al. 2014. Developmental gene expression provides clues to relationships between sponge and eumetazoan body plans. *Nat Commun* 5:3905.

Leys SP, Nichols SA, Adams EDM. 2009. Epithelia and integration in sponges. *Integr Comp Biol* 49:167-177.

Mardones GA, Burgos PV, Brooks DA, Parkinson-Lawrence E, Mattera R, Bonifacino JS. 2007. The trans-golgi network accessory protein p56 promotes long-range movement of GGA/clathrin-containing transport carriers and lysosomal anzyme sorting. *Mol Biol Cell* 18:3486-3501.

McGinnis W, Garber RL, Wirz J, Kuroiwa A, Gehring WJ. 1984. A homologous protein-coding sequence in drosophila homeotic genes and its conservation in other metazoans. *Cell* 37:403-408.

Miller PW, Clarke DN, Weis WI, Lowe CJ, Nelson WJ. 2013. The evolutionary origin of epithelial cell–cell adhesion mechanisms. *Curr Top Membr* 72:267-311.

Momose T, Derelle R, Houliston E. 2008. A maternally localised Wnt ligand required for axial patterning in the cnidarian *Clytia hemisphaerica*. *Development* 135:2105-2113.

Müller WEG, Zahn RK. 1973. Purification and characterization of a species-specific aggregation factor in sponges. *Exp Cell Res* 80:95-104.

Nakanishi N, Sogabe S, Degnan B. 2014. Evolutionary origin of gastrulation: insights from sponge development. *BMC Biol* 12:26.

Nichols SA, Dirks W, Pearse JS, King N. 2006. Early evolution of animal cell signaling and adhesion genes. *Proc Natl Acad Sci U S A* 103:12451-12456.

Nichols SA, Roberts BW, Richter DJ, Fairclough SR, King N. 2012. Origin of metazoan cadherin diversity and the antiquity of the classical cadherin/ $\beta$ -catenin complex. *Proc Natl Acad Sci U S A* 109:13046-13051.

Nickel M, Scheer C, Hammel JU, Herzen J, Beckmann F. 2011. The contractile sponge epithelium *sensu lato* – body contraction of the demosponge *Tethya wilhelma* is mediated by the pinacoderm. *J Exp Biol* 214:1692-1698.

Oda H, Akiyama-Oda Y, Zhang S. 2004. Two classic cadherin-related molecules with no cadherin extracellular repeats in the cephalochordate amphioxus: distinct adhesive specificities and possible involvement in the development of multicell-layered structures. *J Cell Sci* 117:2757-2767.

Oda H, Tsukita S. 1999. Nonchordate classic cadherins have a structurally and functionally unique domain that is absent from chordate classic cadherins. *Dev Biol* 216:406-422.

Oda H, Wada H, Tagawa K, Akiyama-Oda Y, Satoh N, Humphreys T, Zhang S, Tsukita S. 2002. A novel amphioxus cadherin that localizes to epithelial adherens junctions has an unusual domain organization with implications for chordate phylogeny. *Evol Dev* 4:426-434.

Pang K, Ryan JF, Comparative Sequencing Program NISC, Mullikin JC, Baxevanis AD, Martindale MQ. 2010. Genomic insights into Wnt signaling in an early diverging metazoan, the ctenophore *Mnemiopsis leidyi*. *EvoDevo* 1:10.

Peña JF, Alié A, Richter DJ, Wang L, Funayama N, Nichols SA. 2016. Conserved expression of vertebrate microvillar gene homologs in choanocytes of freshwater sponges. *EvoDevo* 7:13.

Riesgo A, Farrar N, Windsor PJ, Giribet G, Leys SP. 2014. The analysis of eight transcriptomes from all Porifera classes reveals surprising genetic complexity in sponges. *Mol Biol Evol* 31:1102-1120.

Sastry SK, Burridge K. 2000. Focal adhesions: A nexus for intracellular signaling and cytoskeletal dynamics. *Exp Cell Res* 261:25-36.

Schneider SQ, Finnerty JR, Martindale MQ. 2003. Protein evolution: structure-function relationships of the oncogene  $\beta$ -catenin in the evolution of multicellular animals. *J Exp Zool B Mol Dev Evol* 295B:25-44.

Schuster A, Vargas S, Knapp I, Pomponi SA, Toonen RJ, Erpenbeck D, Woerheide G. unpublished data. Divergence times in demosponges (Porifera): first insights from new mitogenomes and the inclusion of fossils in a birth-death clock model.  
bioRxiv:doi.org/10.1101/159806.

Shapiro LW, William I. 2009. Structure and biochemistry of cadherins and catenins. *Cold Spring Harb Perspect Biol* 1:a003053.



Srivastava M, Simakov O, Chapman J, Fahey B, Gauthier MEA, Mitros T, Richards GS, Conaco C, Dacre M, Hellsten U, et al. 2010. The *Amphimedon queenslandica* genome and the evolution of animal complexity. *Nature* 466:720-726.

Stehbens S, Wittmann T. 2012. Targeting and transport: How microtubules control focal adhesion dynamics. *J Cell Biol* 198:481-489.

Technau U, Rudd S, Maxwell P, Gordon PMK, Saina M, Grasso LC, Hayward DC, Sensen CW, Saint R, Holstein TW, et al. 2005. Maintenance of ancestral complexity and non-metazoan genes in two basal cnidarians. *Trends Genet* 21:633-639.

Valenta T, Hausmann G, Basler K. 2012. The many faces and functions of  $\beta$ -catenin. *EMBO J* 31:2714-2736.

Wikramanayake AH, Hong M, Lee PN, Pang K, Byrum CA, Bince JM, Xu R, Martindale MQ. 2003. An ancient role for nuclear  $\beta$ -catenin in the evolution of axial polarity and germ layer segregation. *Nature* 426:446-450.

Windsor PJ, Leys SP. 2010. Wnt signaling and induction in the sponge aquiferous system: evidence for an ancient origin of the organizer. *Evol Dev* 12:484-493.

Zihni C, Mills C, Matter K, Balda MS. 2016. Tight junctions: from simple barriers to multifunctional molecular gates. *Nat Rev Mol Cell Biol* 17:564-580.

## FIGURE LEGENDS

**Figure 1. Domain architecture of Em $\beta$ catenin.** The core contains 12 predicted Arm repeats flanked by N- and C-terminal regions. The N-terminal has conserved GSK3 $\beta$  and CKI phosphorylation residues and a putative  $\alpha$ -catenin binding site. Also critical cadherin binding residues are conserved.

**Figure 2. Em $\beta$ catenin antibody specificity.** (A) Western Blot of *E. muelleri* whole-cell lysate. (B) Western blot of precipitate and unbound fractions from IP with anti-Em $\beta$ catN compared to IP with IgG control.

**Figure 3. Em $\beta$ catenin co-localizes with plaques of F-actin at cell contacts in the apical endopinacoderm (AEP).** Composite images (A/B) with DNA (A'/B') in blue, anti-Em $\beta$ catN (A''/B'') in green, and F-actin (A'''/B''') in red. Arrowheads indicate Em $\beta$ catenin enrichment at sites of cell-cell contact. Scale bar: 10  $\mu$ m. (C) Illustrative cross section of *E. muelleri* with AEP in red.

**Figure 4. Em $\beta$ catenin localization in the attachment epithelium at cell boundaries and at FAs.** Composite images (A) with DNA (A') in blue, anti-Em $\beta$ catN (A'') in green, and F-actin (A''') in red. Arrow indicates Em $\beta$ catenin enrichment at cell boundaries and open arrowhead indicates Em $\beta$ catenin enrichment at FA. Scale bar: 10  $\mu$ m. (B) Illustrative cross section of *E. muelleri* with attachment epithelium in red.

**Figure 5. Nuclear localization of Em $\beta$ catenin in migratory cells in the mesohyl.** Composite images (A) with DNA (A') in blue, anti-Em $\beta$ catN (A'') in green, and F-actin (A''') in red. Scale bar: 10  $\mu$ m. (B) Illustrative cross section of *E. muelleri* with migratory cells in mesohyl in red.

**Figure 6. Em $\beta$ catenin co-localizes at cell boundaries in the choanoderm.** Composite images (A/B/C) with DNA (A'/B'/C') in blue, anti-Em $\beta$ catN (A''/B''/C'') in green, and F-actin (A'''/B'''/C''') in red. Arrows indicate Em $\beta$ catenin enrichment at cell boundaries. Scale bar: 10  $\mu$ m. (D) Illustrative cross section of *E. muelleri* with choanoderm in red.

**Figure 7. Nuclear localization of Em $\beta$ catenin in cells of the leading edge of the attachment epithelium.** Composite images (A/B) with DNA (A'/B') in blue, anti-Em $\beta$ catenin (A''/B'') in green, and F-actin (A'''/B''') in red. Scale bar: 10  $\mu$ m. (C) Illustrative cross section of *E. muelleri* with leading edge of the attachment epithelium in red.

**Figure 8. Western blot showing effect of AP and BIO on phosphorylated Em $\beta$ -catenin protein levels from sponge cell lysate.** Open arrowhead: GSK3 $\beta$  - phosphorylated Em $\beta$ catenin; closed arrowhead: active Em $\beta$ catenin (i.e. unphosphorylated); asterisk: minimal effective dosage of AP and BIO which results in a complete shift from phosphorylated to active Em $\beta$ -catenin.

**Figure 9.** The effect on sponge morphology after treating the sponges with the minimal effective dose of the drugs AP (0.1  $\mu$ M) and BIO (1  $\mu$ M). Canals and choanoderm did not develop.

## TABLES

**Table 1. Mass spectrometry results of Co-IP**

Identity	T-PEP ID	Summed # unique peptides	Summed # total spectrum	MW (kDa)
<b>Em<math>\beta</math>catenin</b>	m.48575	32	104	98
<b>ccdc-91/p56</b>	m.42889	14	22	79
<b>EmCDH2</b>	m.5230 / m.46898	10	12	587
<b>Em<math>\alpha</math>-catenin</b>	m.75406	5	11	102

## FIGURES

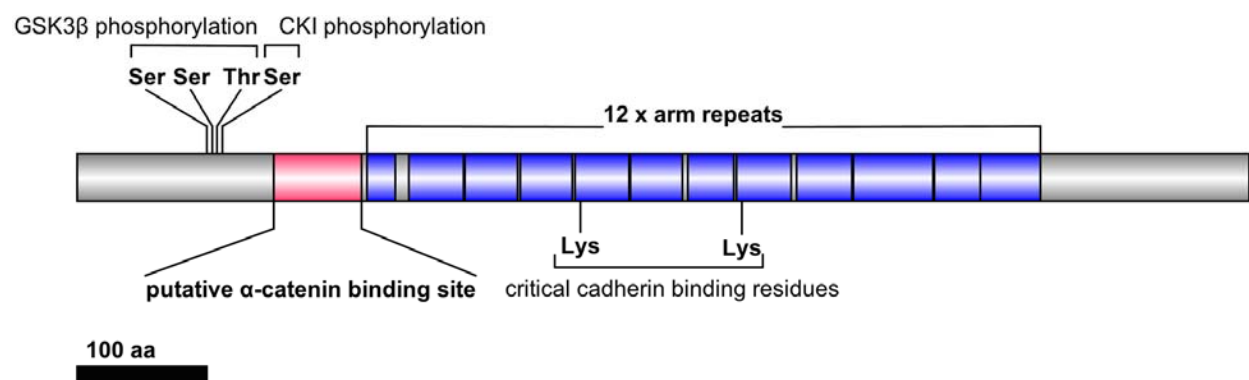


Figure 1

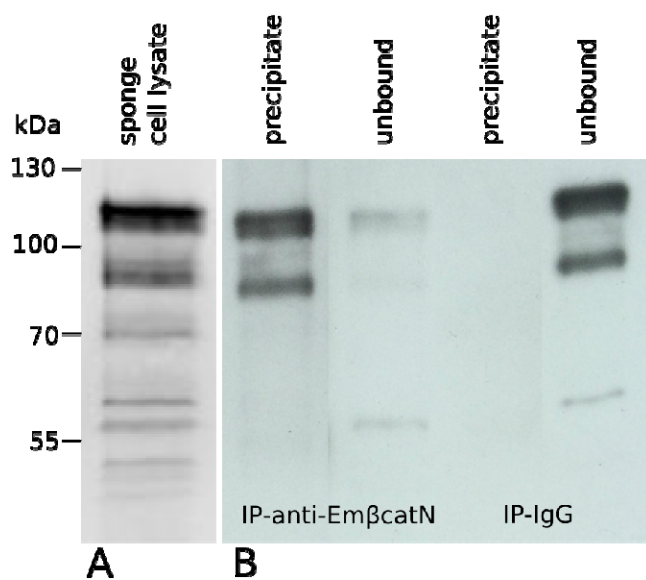


Figure 2

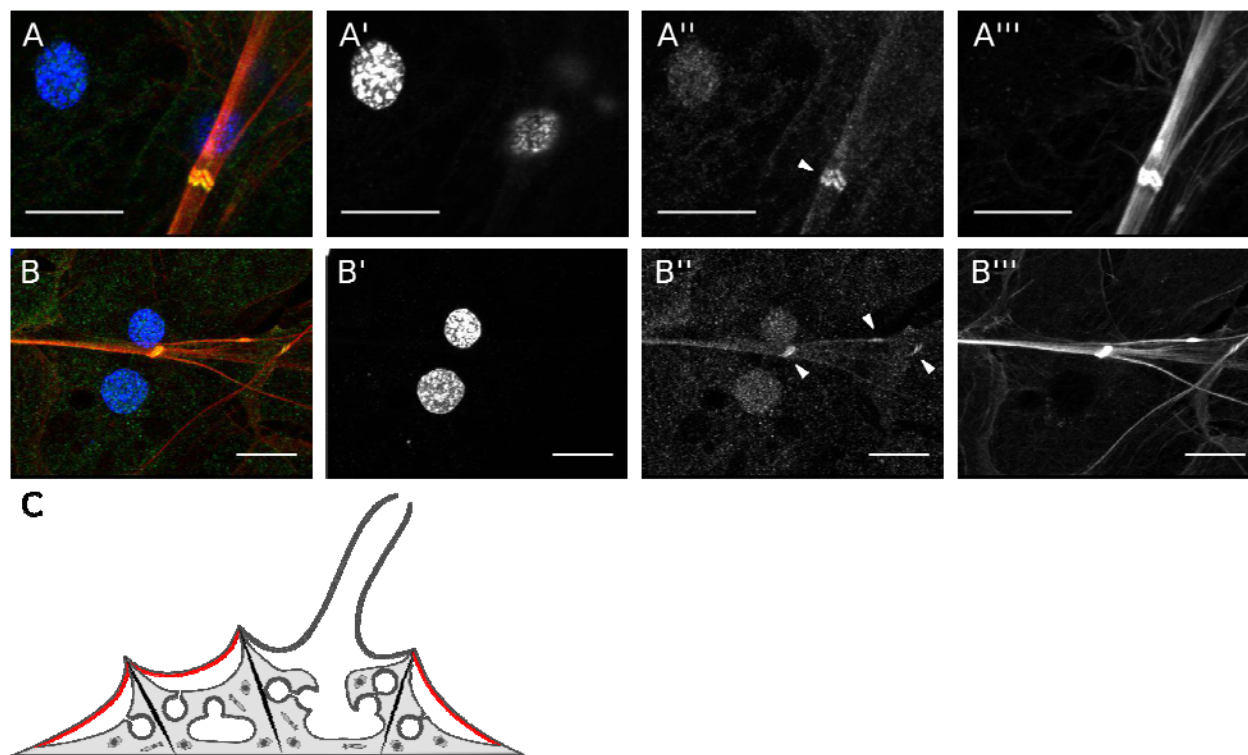


Figure 3

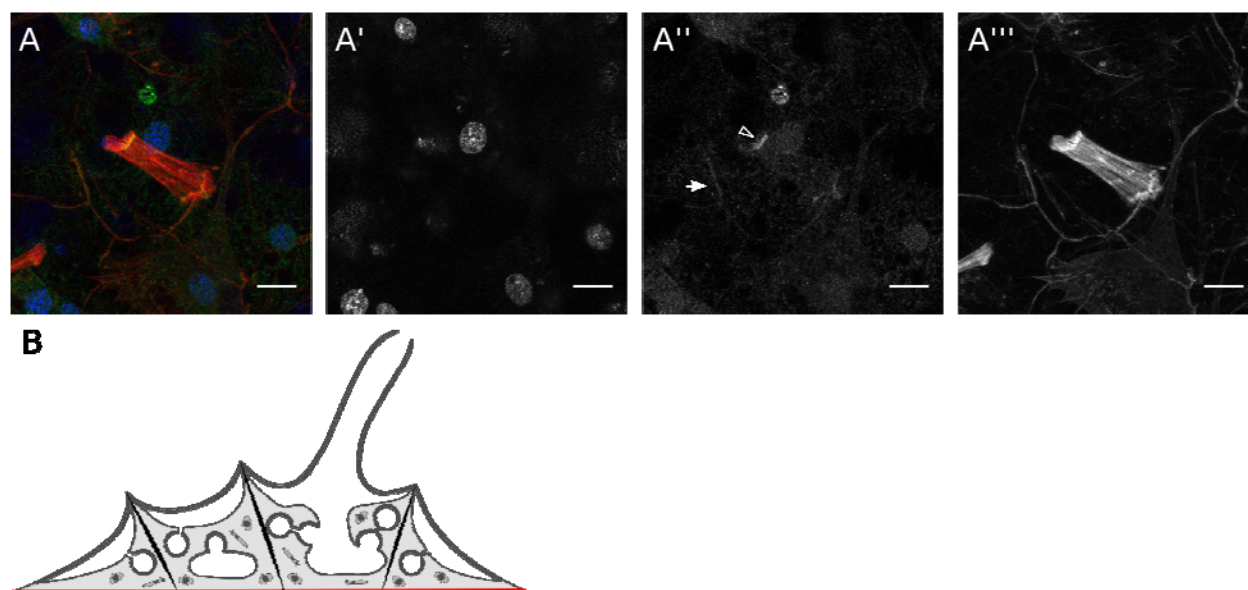


Figure 4

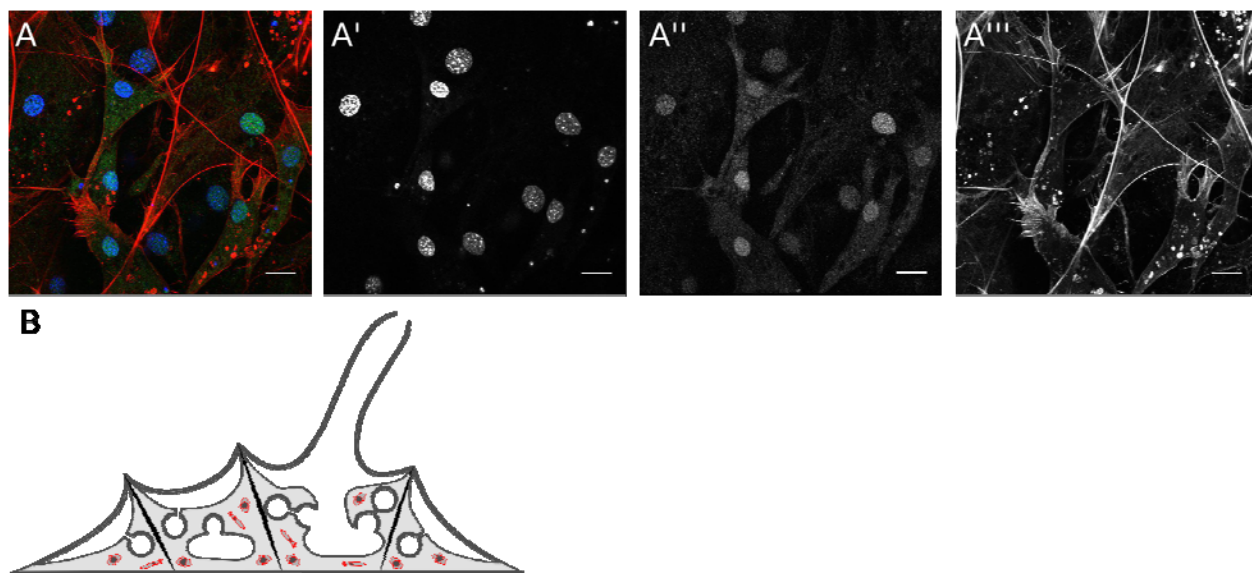


Figure 5

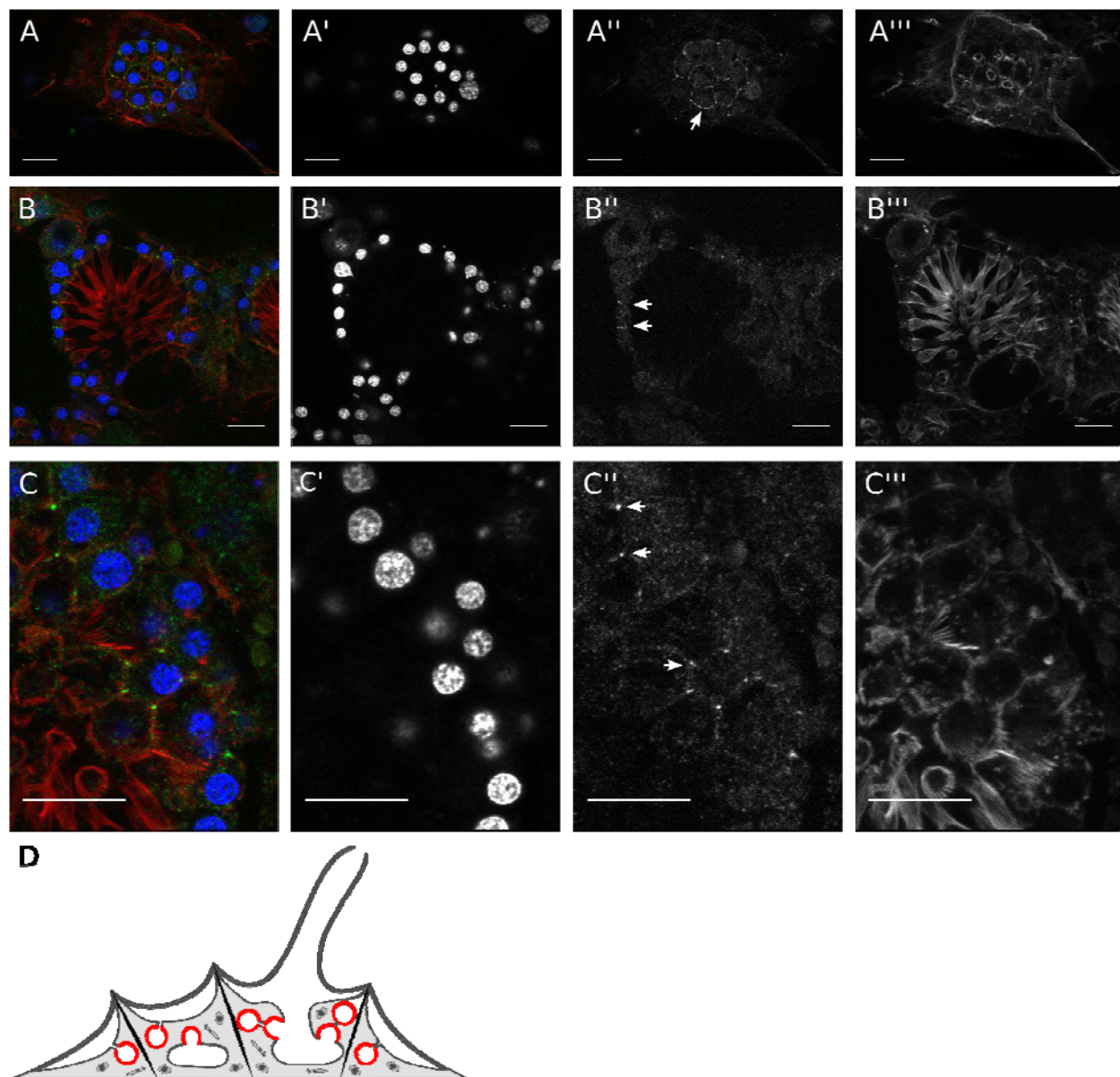


Figure 6



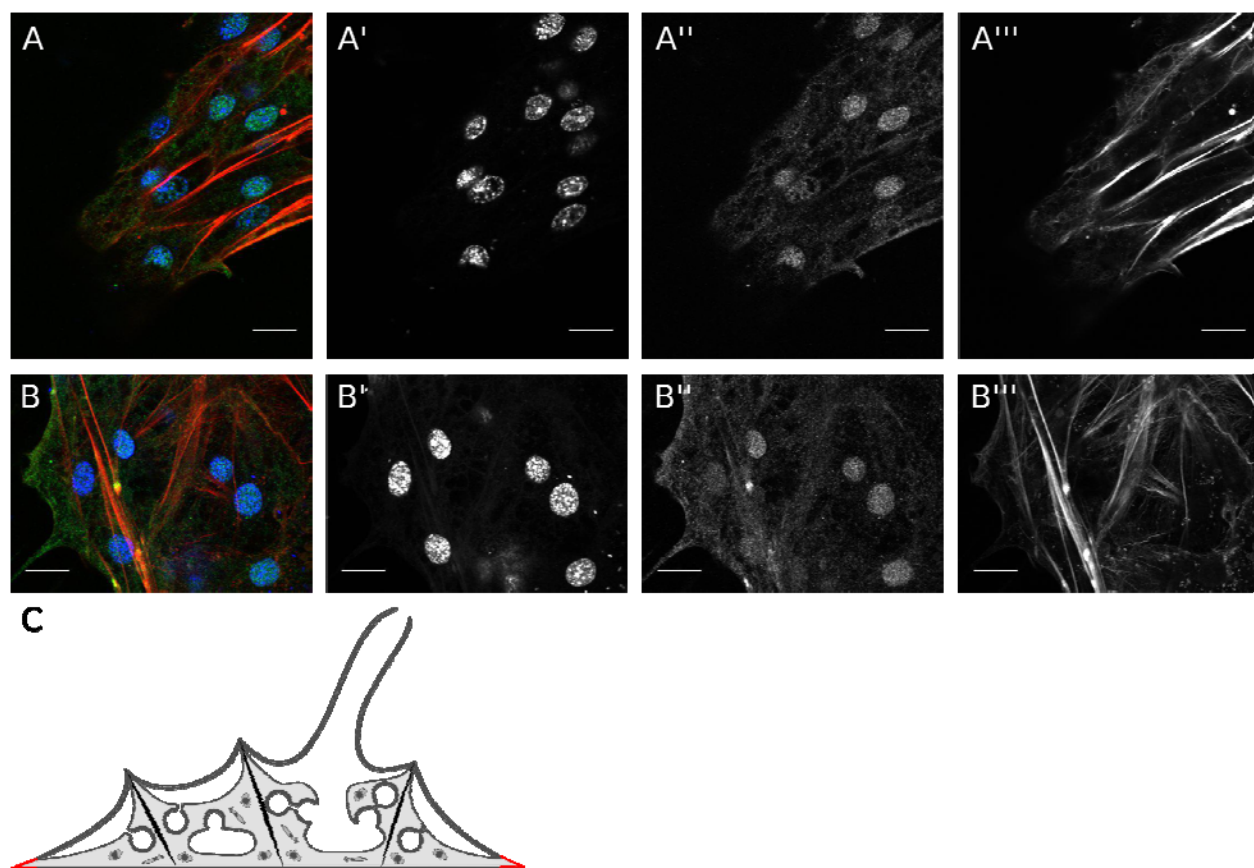


Figure 7

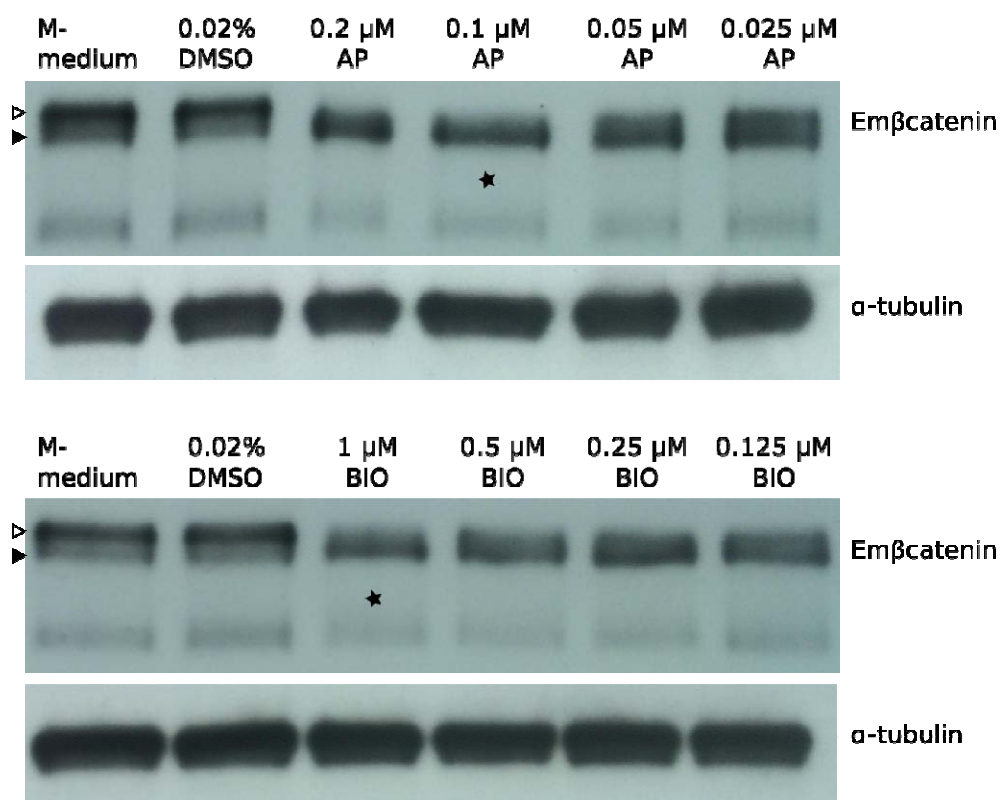


Figure 8

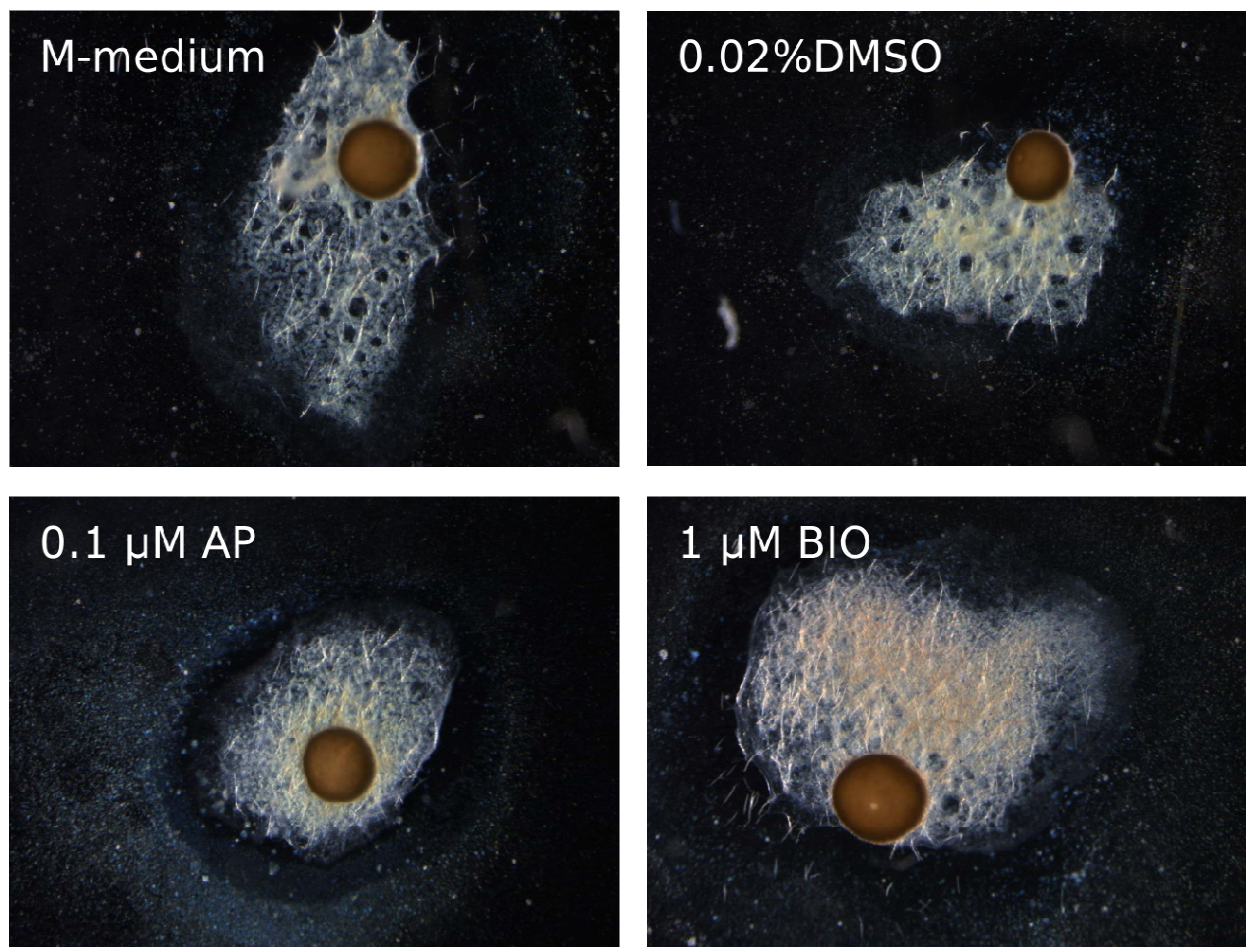


Figure 9